International Immunopharmacology 11 (2011) 187–193

Contents lists available at ScienceDirect

International Immunopharmacology

journal homepage: www.elsevier.com/locate/intimp

Heparin changes the conformation of high-mobility group protein 1 and decreases its affinity toward receptor for advanced glycation endproducts *in vitro*

Yan Ling, Zhi-Yong Yang, Tao Yin, Li Li, Wei-Wei Yuan, He-Shui Wu, Chun-You Wang *

Pancreatic Surgery, Union Hospital, Tongji Medical College, Huazhong University of Science and Technology, Wuhan, Hubei Province 430022, China

ARTICLE INFO

Article history:
Received 17 March 2010
Received in revised form 4 November 2010
Accepted 4 November 2010
Available online 21 November 2010

Keywords:
High-mobility group protein 1 (HMGB1)
Receptor for advanced glycation end products (RAGE)
Heparin
Affinity analysis
Fluorescence spectrometry
Surface plasmon resonance (SPR) technique

ABSTRACT

High-mobility group protein 1 (HMGB1) has been identified as a late-acting mediator of inflammation. The receptor for advanced glycation end products (RAGE) is the main receptor and mediates the cytokine activity of HMGB1. Since HMGB1 also exhibits heparin-binding activity, we investigated whether heparin interferes with HMGB1/RAGE interaction and prevents the cytokine activity. We used fluorescence spectrometry, circular dichroism spectrometry and SPR biosensor technique to evaluate the effect. After treatment of HMGB1 with different concentrations of heparin (0, 50, 100 and 1000 U/L), the fluorescence peak values of HMGB1 increased and the emission wavelength showed red shifts; further, the secondary structure of HMGB1 showed a marked change in that the content of β-pleated sheet reduced while that of α-helix increased. The equilibrium dissociation constants (K_D) were determined by SPR technique; $K_D = 4.5 \times 10^{-9}$ mol/L for heparin and HMGB1 and $K_D = 9.77 \times 10^{-8}$ mol/L for HMGB1 and RAGE, respectively. Heparin and RAGE had no interaction. The amount of HMGB1 and RAGE bound forms reduced after treatment with heparin. ELISA revealed that addition of heparin inhibited the TNF-α and IL-6 released by macrophages RAW264.7 and HUVEC; 10 U/L and 50 U/L of heparin showed the most marked inhibitory effect in RAW264.7 cells and in HUVEC, respectively. In conclusion, heparin can combine with HMGB1 and affect the affinity of HMGB1/RAGE by changing the conformation of HMGB1. And this effect was independent of heparin concentration, so that a low dose of heparin was sufficient to achieve the best anti-inflammatory effect in our test.

1. Introduction

Sepses, diabetes, rheumatic arthritis, sever acute pancreatitis and so on are common, and are high risk for human health. And the systemic inflammatory response syndrome (SIRS) occurred during the diseases is still a problem that disturbs the treatment and the high-mobility group protein 1 (HMGB1) was found playing a vital role in the progress.

The high-mobility group protein 1 (HMGB1), which is also known as P30, amphoterin, or HMG-1, is a highly conserved protein and shows above 99% amino acid homology between HMGB1 of human beings and that of rodents [1]. This protein has a highly dipolar structure: it contains a 185-amino acid basic region and a 30-amino acid cluster of acidic residues at the C-terminus; the band of this protein migrates to the 30 kDa position on a standard polyacrylamide electrophoresis gel. The 185-amino acid basic part is subdivided into 2 homologous HMG boxes, namely, box A and box B, each around 75 amino acids in length. Both the boxes have a similar α-helical structure to allow DNA binding [2,3]. The three-dimensional structure of the whole HMGB1 molecule has not been elucidated to date. The N-terminus of HMGB1 (residues 6–12) contains a consensus sequence that has also been identified in several heparin-binding proteins [4], which likely contributes to the heparin-binding ability of HMGB1. The region between the HMG-box B and the acidic tail of HMGB1 (residues 151–183) is the most distinctive feature of HMGB1 in comparison with the characteristics of the other members of the HMG protein family. This region of HMGB1 contains a motif that can bind to receptor for advanced glycation end products (RAGE) [5]. The highly acidic C-terminus of HMGB1 plays an important role in nuclear functions [6,7]. The proinflammatory activity of HMGB1 is localized to the HMG-box B, especially to the residues 89–108 [8].

HMGB1 is a nonhistone DNA-binding protein; it is involved in stabilizing nucleosome formation, increasing gene transcription, and modulating steroid hormone receptors [9,10]. Recently, HMGB1 has been identified as the late-acting mediator of endotoxin lethality [11]. When released from cells, HMGB1 can bind to cell-surface receptors [e.g., RAGE, Toll-like receptor (TLR) (TLR2 and TLR4)] and mediate the chemotactic cell movement and the release of proinflammatory cytokines [e.g., tumor necrosis factor (TNF) and interleukin (IL)-1] [12,13].

RAGE is expressed in endothelial cells, vascular smooth muscle cells, neurons, and macrophages/monocytes [14] and it is the main HMGB1 receptor. RAGE is a 50 kDa protein (404 amino acids in the protein sequence of humans) and belongs to a member of the immunoglobulin superfamily of cell-surface molecules. This protein is composed of an extracellular region containing 1 V-type immunoglobulin (Ig) domain

* Corresponding author.
E-mail addresses: lingyan1029@163.com (Y. Ling), chunyouwang52@126.com (C.-Y. Wang).

1567-5769/$ – see front matter.
doi:10.1016/j.intimp.2010.11.014

and 2 C-type Ig domains; a hydrophobic transmembrane-spanning domain; and a highly charged short cytoplasmic domain [15]. The ligand-binding properties of RAGE can be attributed to the distal V-type domain that contains 2 potential N-glycosylation sites [16].

Heparin, a highly sulfated glycosaminoglycan, has been used as an anticoagulant for clinical purposes for more than 70 years. It has been recently discovered that heparin possesses anti-inflammatory activity; however, the mechanisms of this activity remain to be determined. In our previous research, we have found that heparin inhibits the proinflammatory activity of HMGB1. Heparin interferes with the specific binding of HMGB1 with RAGE by causing conformation changes in HMGB1. In this study, we evaluated the effect of heparin on HMGB1 and investigated the underlying mechanisms. Here, we provided a novel therapeutic method and an evidence for using heparin and its analogues in treatment of inflammatory reaction.

2. Materials and methods

2.1. Equipment and reagents

2.1.1. Equipment

Fluorescence spectrometer FP-6500 and circular dichroism (CD) spectropolarimeter J-810 were from JASCO (Tokyo, Japan); surface plasmon resonance (SPR) measurements were performed on a BIAcore 3000 system from BiacoreAB (Uppsala, Sweden) by using the BIAcore evaluation software version 4.0.

2.1.2. Reagents

HMGB1 and heparin were purchased from Sigma-Aldrich (USA); RAGE (membrane bound derivative) was purchased from R&D systems (USA). Fluorescence spectrometry and CD spectropolarimetry analysis were performed using 0.05 M Tris–HCl buffer (pH 7.4) containing 0.10 M NaCl to maintain the ionic strength. The BIAcore research-grade sensor chip CM5 (composed of carboxymethylated dextran coupled to gold-coated glass surface and prepared according to procedures described elsewhere), amine-coupling kit [containing *N*-ethyl-*N*-(dimethyaminopropyl) carbodiimide (EDC), *N*-hydroxysuccinimide (NHS), and a solution of 1 M ethanol amine hydrochloride whose pH was adjusted to 8.5 using sodium hydroxide], and HBS-EP buffer (10 mM HEPES, 150 mM NaCl, 3 mM EDTA, and 0.005% P20; pH 7.4) were purchased from BiocoreAB (Uppsala, Sweden). Medium 1640 was purchased from Hyclone (USA). ECM (endothelial cell medium) was purchased from Sciencell (USA). All solutions were filtered through 0.22-μm Watman filters and degassed (Milipore sintered glass funnel) before use. All experiments were conducted at 25 °C.

2.2. Experimental methods

2.2.1. Fluorescence spectroscopy and synchronous fluorescence spectroscopy analysis of HMGB1

Steady-state fluorescence measurements were obtained using a FP-6500 spectrophotometer equipped with a 0.1-cm quartz cell. HMGB1 (0.025 g/L) was mixed with different heparin concentrations of 0, 50, 100, and 1000 U/L. The samples were incubated at 25 °C for 15 min before further analysis. The excitation wavelength was 280 nm, the width of the excitation and emission slits was 3 nm, and the scanning speed was 500 nm/min. Synchronous scanning fluorescence spectra were recorded as described by Rao [17]. The excitation and the emission wavelengths (λ_{ex} and λ_{em}) for synchronous fluorescence measurements were scanned simultaneously with a constant wavelength interval ($\Delta\lambda = 15$ nm and $\Delta\lambda = 60$ nm) between λ_{ex} and λ_{em} and with the speed of 500 nm/min.

2.2.2. CD spectroscopy of HMGB1

The wavelengths in the CD spectrum (range, 190–250 nm) were recorded using a quartz cuvette with a path length of 10 mm. The scanning speed was 1000 nm/min. The samples were prepared according to the abovementioned method. Each sample was analyzed 3 times, and the conformation of the unit was calculated according to Chen–Yang's method [18].

2.2.3. Immobilization of HMGB1 and RAGE on CM5 sensor chip surface

Standard BIAcore amine-coupling protocol involving EDC and NHS was applied. HMGB1 was diluted with 10 nM sodium acetate (pH 5.0) to the concentration of 50 mg/L, and RAGE was diluted with 10 nM sodium acetate (pH 4.5) to the concentration of 40 mg/L. The concentrations of stock EDC/NHS solutions were 0.2 M and 0.05 M, respectively. The flow cells (Fc) 2 and Fc4 contained immobilized HMGB1 and RAGE, respectively, while Fc1 and Fc3 were used as negative controls.

2.2.4. Analysis of heparin–HMGB1 and HMGB1–RAGE interactions

Heparin samples of different concentrations were diluted with HBS-EP and 20-μL aliquots of this solution were injected over Fc2 on CM5 sensor chip at a flow rate of 30 μL/min. Next, HMGB1 samples of different concentrations were diluted with HBS-EP and 20-μL aliquots were injected over Fc4 at a flow rate of 30 μL/min. At the end of injection, HBS-EP buffer was allowed to flow freely over the sensor surface to facilitate disassociation. After a 2-min dissociation time, the sensor surface was regenerated by injecting 10 mM NaOH. Each cycle included a 2 min break time to allow the monitoring of baseline stability. All Biacore data were collected at pH 7.4 by using HBS-EP as the running buffer and a constant flow rate of 30 μL/min.

2.2.5. SPR binding analysis

HMGB1 diluted with 50 mg/L HBS-EP was injected over the chip surface for 3 min; after a 150-s dissociation period, HMGB1 plus heparin (50, 100, 1000, and 10,000 U/L) solutions were injected over the chip surface for 3 min in the given order of concentrations. Then, the chip surface was regenerated by injecting 10 mM NaOH. All data were collected with running buffer and at a constant flow rate of 20 μL/min.

2.2.6. SPR data analysis

When performing binding assays for heparin–HMGB1 and HMGB1–RAGE by using the BIAcore 3000 system, the binding-response signals were continuously recorded in response units (RU) and presented graphically as the function of time. The BIAcore 3000 system uses a flow-injection system and allows the running buffer to flow over the chip surface at a constant flow rate. Hence, it could be presumed that the concentrations of the samples were constant. Therefore, we adopted the 1:1 (Langmuir) binding fitting model in which the association (ka) and dissociation (kd) constants are fitted simultaneously using Eq. (1) [19]:

$$dR/dt = ka.C(R_{max}-R)-kdR, \quad (1)$$

where R represents the response unit; C is the concentration of ligand (heparin or HMGB1); and R_{max} stands for the maximal response. The affinity constant (K_A) and the equilibrium dissociation constant (K_D) could be obtained from ka and kd by using the following relations:

$$K_A = ka/kd \quad K_D = kd/ka. \quad (2)$$

2.2.7. Detection of TNF-α and IL-6 in cell supernatant

Intact RAW 264.7 macrophages were added to medium 1640 (10% fetal calf serum or FCS) and cultured in 24-hole plate at a density of 4×10^4 in 37 °C and 5% CO_2 for 24 h; subsequently, this medium was replaced by serum-free opti-MEM medium and the cells were incubated for another 24 h. The cells were stimulated with HMGB1 (0.1 μg/mL) and different concentrations of heparin (0.1 U/L, 1 U/L, and 10 U/L) at

different time points 0, 1, 2, 3, 6, 9, 12 and 15 h. Finally, the supernatants were collected, centrifuged, and the resulting supernatants were used to determine the presence of TNF-α and IL-6 by ELISA. The tests were repeated 3 times.

Intact HUVEC were added to medium ECM (5% fetal calf serum) and cultured as abovementioned. The cells were stimulated with HMGB1 (0.1 μg/mL) and different concentrations of heparin (0.1 U/L, 1 U/L, 10 U/L, 50 U/L, 100 U/L, 1000 U/L and 10,000 U/L) for 24 h. Finally, the supernatants were used to determine the presence of TNF-α and IL-6 by ELISA. The tests were repeated 3 times.

2.2.8. Statistical analysis

The data were expressed as $\bar{x} \pm s$ and were compared using Independent-Samples *T* test for independent groups. Analysis was performed by *SPSS 13.0* software and considered statistically significant when P value was less than 0.05.

3. Results

3.1. Fluorescence spectrometry analysis of heparin and HMGB1

The fluorescence intensity of only HMGB1 was high, but the intensity of the mixture of HMGB1 and heparin of concentrations 0 U/L–1000 U/L (Fig. 1A) was low. After mixing with heparin, an increase was observed in the intensity peak value. Interestingly, 50 U/L heparin had the most marked effect on the fluorescence intensity, rather than 1000 U/L heparin, which was the highest concentration.

Among the amino acids constituting proteins, only tyrosine, tryptophan, and phenylalanine exhibit fluorescence on excitation. Phenylalanine transfers its energy by way of resonance transfer to tryptophan; therefore, phenylalanine does not show a fluorescence emission peak [20]. In a normal fluorescence spectrum, the emission peaks of tryptophan and tyrosine are overlapped and they cannot be discerned. Synchronous fluorescence spectroscopy with an appropriate wavelength (Δλ) can be used to separate the fluorescence peaks and afford the characteristic peaks of tryptophan and tyrosine.

When Δλ = 15 nm was used, the highest fluorescence peak was obtained at 297 nm (Fig. 1B), and when Δλ 60 nm was used, 2 fluorescence peaks were obtained at 292 nm and 332 nm (Fig. 1C). Mainly, the microenvironment of the protein contributed to the fluorescence intensities corresponding to Δλ = 15 nm and Δλ = 60 nm [21]. Hence, in our results, the peak obtained at 292 nm was the characteristic of tyrosine and that obtained at 332 nm was the characteristic of tryptophan.

The synchronous fluorescence spectral patterns were similar to the fluorescence spectral patterns at Δλ = 15 nm and Δλ = 60 nm. When Δλ was 15 nm, the wavelength corresponding to the fluorescence peak did not change, but when Δλ was 60 nm, the wavelength showed a red shift of 2 nm for the sample containing 50 U/L heparin (Fig. 2A and B).

3.2. CD spectroscopy and changes in the secondary structure

CD spectroscopy is a commonly used method to study protein conformation. Because of the relationship between CD and the absorption peak, this technique is useful to interpret protein conformation [22]. Hence, we can use CD spectroscopy to measure the absorption peaks of the samples (figure not shown); further, in accordance with Chen–Yang's methods [18], we can calculate the contents of the conformation units (Table 1).

After the addition of heparin, HMGB1 showed a change in the secondary structure: the content of α-helix increased while that of β-pleated sheet reduced. The most remarkable change was observed in the sample containing 50 U/L heparin (Table 1).

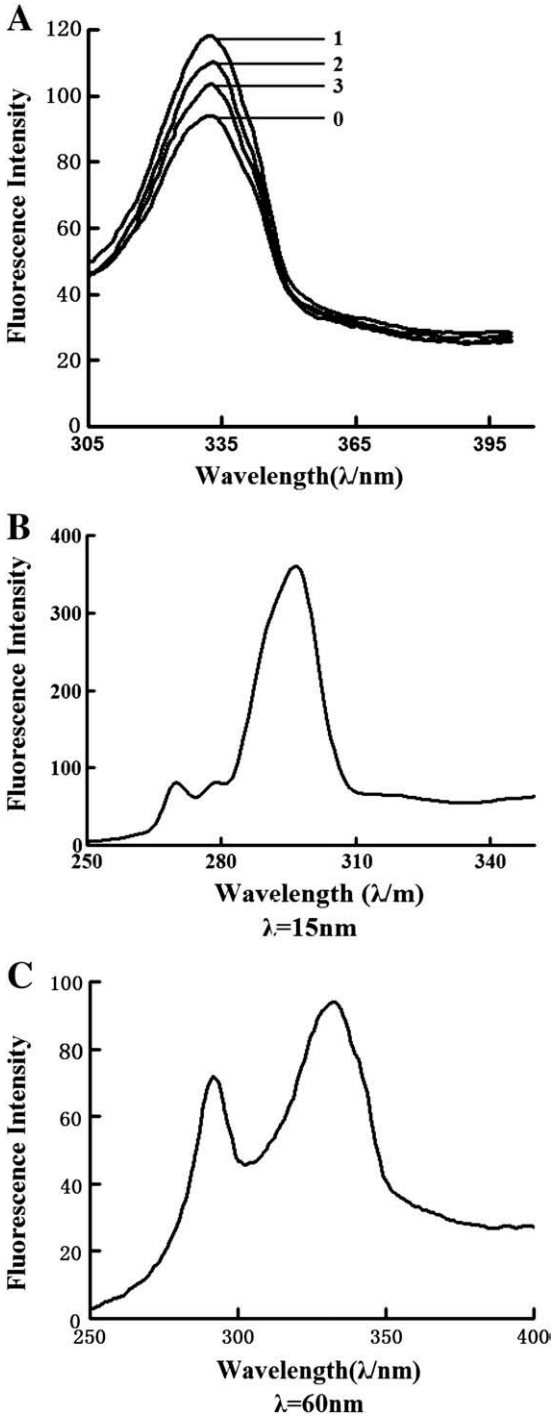

Fig. 1. Fluorescence spectra of HMGB1 and heparin mixture and synchronous fluorescence spectra of HMGB1 when Δλ = 15 nm and Δλ = 60 nm. (A) After incubated with different concentrations of heparin (0, 50, 100, and 1000 U/L), the fluorescence intensities of HMGB1 (0.025 g/L) were recorded. (B) Synchronous fluorescence intensity of HMGB1 (0.025 g/L) was recorded in Δλ = 15 nm and got a peak value at 297 nm. (C) Synchronous fluorescence intensity of HMGB1 (0.025 g/L) was recorded in Δλ = 60 nm and got two peak values at 292 nm and 332 nm.

3.3. Immobilization of HMGB1 and RAGE on CM5 sensor chip

At the end of the immobilization, we obtained a 9000 RU increase in the HMGB1 signal, which represents the amount of immobilized HMGB1, and a 5000 RU increase in the RAGE signal. Moreover, Stenberg [23] have reported that 1000 RU corresponds to approximately 1 ng/mm^2 change in protein concentration on the chip surface. Accordingly, in this experiment, the concentration of immobilized

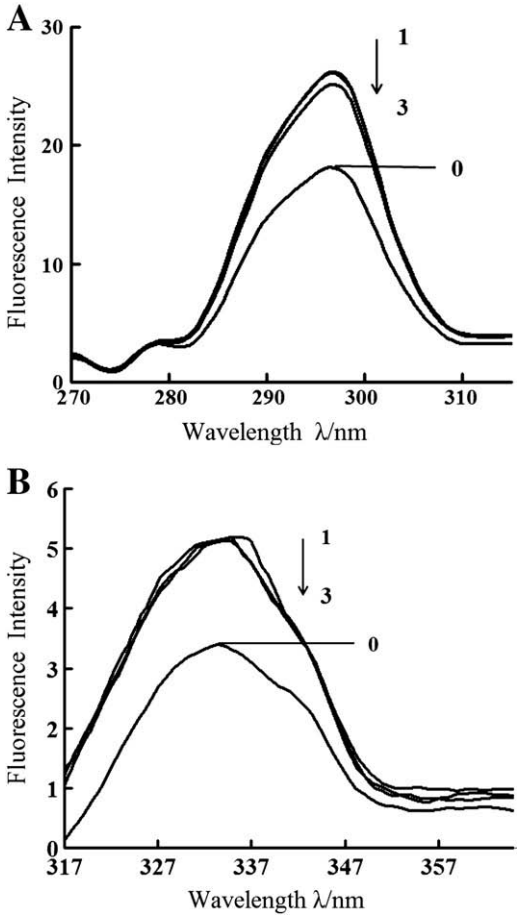

Fig. 2. Synchronous fluorescence spectrometry of HMGB1 mixed with heparin when $\Delta\lambda = 15$ nm (A) and $\Delta\lambda = 60$ nm (B). After incubation with different levels of heparin (0, 50, 100, and 1000 U/L from 0 to 3), (A) synchronous fluorescence intensities of HMGB1 (0.025 g/L) were recorded at $\Delta\lambda = 15$ nm. The peak values from 0 to 3 were 18.10, 26.17, 26.15 and 25.12 respectively. (B) Synchronous fluorescence intensity of HMGB1 was scanned at $\Delta\lambda = 60$ nm. The peak values from 0 to 3 were 3.39, 5.20, 5.18 and 5.13 respectively. And the emission wavelength showed a red shift of about 2 nm. The results were expressed as $\bar{x} \pm s$ of 3 independent experiments.

HMGB1 was approximately 9 ng/mm^2 and that of immobilized RAGE was 5 ng/mm^2.

3.4. Analysis of heparin–HMGB1 interaction kinetics

Heparin–HMGB1 interaction was investigated based on the biosensor chip response after the initiation of heparin injections (Fig. 3A). The different constants were evaluated using the BIAevaluation 4.0 software assuming the 1:1 interaction (Langmuir model) between the immobilized ligand (HMGB1) and the soluble analyte (heparin); kinetic constants were $ka = 1.78 \times 10^5\ L \cdot mol^{-1} \cdot s^{-1}$ and $kd = 8.02 \times 10^{-4}\ s^{-1}$; affinity constant was $K_A = 2.22 \times 10^8\ L \cdot mol^{-1}$; and equilibrium dissociation constant was $K_D = 4.5 \times 10^{-9}\ mol \cdot L^{-1}$. These constants indicated that the immobilization of HMGB1 did not destroy heparin-binding sites on HMGB1, and it did not affect the affinity of heparin toward HMGB1.

Table 1
Effect of heparin on the circular dichroism spectra of HMGB1.

	HMGB1	HMGB1 + 50 U/L	HMGB1 + 100 U/L	HMGB1 + 1000 U/L
Helix	13.2%	20.2%	17.7%	14.2%
Beta	60.5%	48.6%	53.6%	56.7%
Turn + Random	26.2%	31.2%	28.7%	29.0%

Helix, alpha helix; Beta, β-pleated sheet; Turn + Random, β-turn and random coil.

3.5. Analysis of HMGB1–RAGE interaction kinetics

HMGB1–RAGE interaction was examined on the basis of the biosensor chip response after the initiation of HMGB1 injections (Fig. 3B). Assuming the 1:1 interaction (Langmuir model) between the immobilized ligand (RAGE) and soluble analyte (HMGB1), we obtained the kinetic constants $ka = 1.85 \times 10^3\ L \cdot mol^{-1} \cdot s^{-1}$ and $kd = 1.81 \times 10^{-4}\ s^{-1}$; affinity constant, $K_A = 1.02 \times 10^7\ L\ mol^{-1}$; and equilibrium dissociation constant, $K_D = 9.77 \times 10^{-8}\ mol \cdot L^{-1}$. These constants indicated that the immobilization of RAGE did not destroy

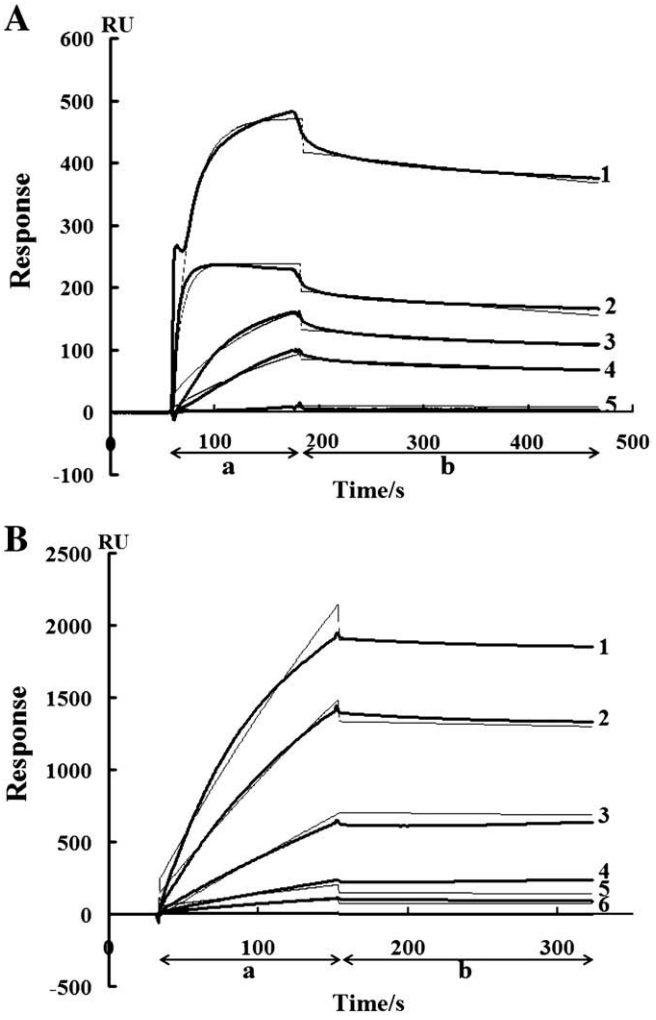

Fig. 3. SPR sensor grams of specific binding of serially diluted heparin to immobilized HMGB1 on the surface of the CM5 sensor chip (A) and of serially diluted HMGB1 to immobilized RAGE on the sensor chip (B). (A) HMGB1 was covalently immobilized onto Fc2 of the biosensor chip CM5 as described before. Twenty-microliter aliquots of heparin of different concentrations (10,000, 1000, 100, 50, and 10 U/L from 1 to 5) were injected on the biosensor surface at a flow rate of 30 μL/min. The running buffer was allowed to flow over the chip surface at a rate of 30 μl/min while heparin dissociated from the surface. Then, the surface was regenerated by injecting 10 mM NaOH. This curve was obtained by subtracting the response signal of Fc2 from that of the reference Fc1 (Fc2–Fc1). Section (a) indicates the association stage and section (b) indicates the dissociation stage. The dissociation constant was calculated based on the 1:1 (Langmuir) binding model. The equilibrium dissociation constant (K_D) of heparin and HMB1 was $4.5 \times 10^{-9}\ mol \cdot L^{-1}$. (B) RAGE was covalently immobilized onto the Fc4 of biosensor chips. Subsequently, different concentrations of HMGB1 (2000, 1000, 500, 250, 125, and 0 nM from 1 to 6) were injected on the biosensor surface at a flow rate of 30 μl/min. This sensorgram is obtained by subtracting the response signal of from Fc4 from that of the referenced Fc3 (Fc4–Fc3). The K_D of HMGB1 and RAGE was $9.77 \times 10^{-8}\ mol \cdot L^{-1}$.

the RAGE-binding sites on HMGB1, and did not affect the affinity of HMGB1 toward RAGE.

3.6. Kinetic analysis of heparin–RAGE interaction

We analyzed heparin–RAGE interaction by the experimental procedure used for analyzing HMGB1–RAGE interaction. We injected heparin (0, 50, 100, 1000, and 10,000 U/L) through Fc4 on which RAGE was immobilized and obtained the sensorgrams of Fc4 and Fc3. The response value was less than 10 RU even for the highest heparin concentration (10,000 U/L). Hence, in this study, heparin and RAGE showed no affinity or very low affinity toward each other (figure not shown).

3.7. Effect of heparin on HMGB1–RAGE affinity

An increase in RU indicated changes in the concentration of molecules at the surface of the sensor chip resulting from a specific interaction between analyte (HMGB1 or HMGB1 mixture with another compound) and ligand (RAGE). The RUs of the mixture of HMGB1 (50 mg/L) and heparin (10,000, 1000, 100, and 50 U/L) were markedly different from the RU of 50 mg/L HMGB1 without any heparin. The changes in the RU values were 55, 62, 50, 48and 2RU from 10,000 U/L to 0 U/L (Fig. 4).

3.8. ELISA for detecting TNF-α and IL-6 in the supernatant

RAW 264.7 macrophages were stimulated after treatment with HMGB1 and different concentrations of heparin; TNF-α (Fig. 5A) concentration reached the peak value in 2 and 12 h and the TNF-α concentration decreased with increasing heparin concentration. The IL-6 (Fig. 5B) concentration also decreased in a dose dependent manner of heparin and the level of 10 U/L reached the most decreasing effect. These results indicate that heparin could inhibit the secretion of TNF-α and IL-6 in macrophages.

As revealed in Fig. 6, the levels of IL-6(Fig. 6A) and TNF-α (Fig. 6B) in supernatant of HUVEC were decreased after incubation with different concentrations of heparin. And heparin could inhibit about 50% effect of HMGB1 ($P<0.05$) at 50 U/L. IL-6 and TNF-α levels increased obviously after the HMGB1 stimulation compared with that without any stimulus ($P<0.01$).

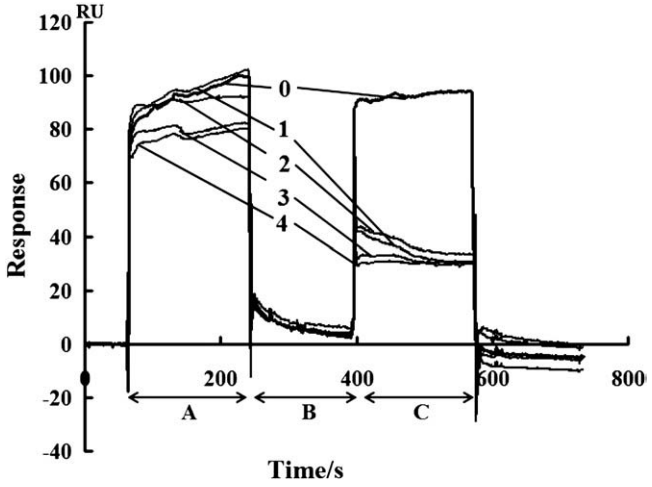

Fig. 4. Sensor grams of specific binding of HMGB1 mixed with serially diluted heparin to immobilized RAGE on the surface of sensor chip. Section (A) indicated the 3 min injection stage of HMGB1 (50 mg/L) to immobilized RAGE. The RU increased immediately once injected. Section (B) demonstrated the 150 s injection interval of running buffer with the RU decreased sharply. Section (C) represented the 3 min injection stage of HMGB1 (50 mg/L) which were mixed with different concentrations of heparin (0, 10,000, 1000, 100, and 50 U/L from 0 to 4). The changes in ΔRU values were 2, 55, 62, 50and 48 from 0 to 4. Compared with the values in section A, the RU values decreased obviously, and it represented that the combination of HMGB1 with immobilized RAGE had declined.

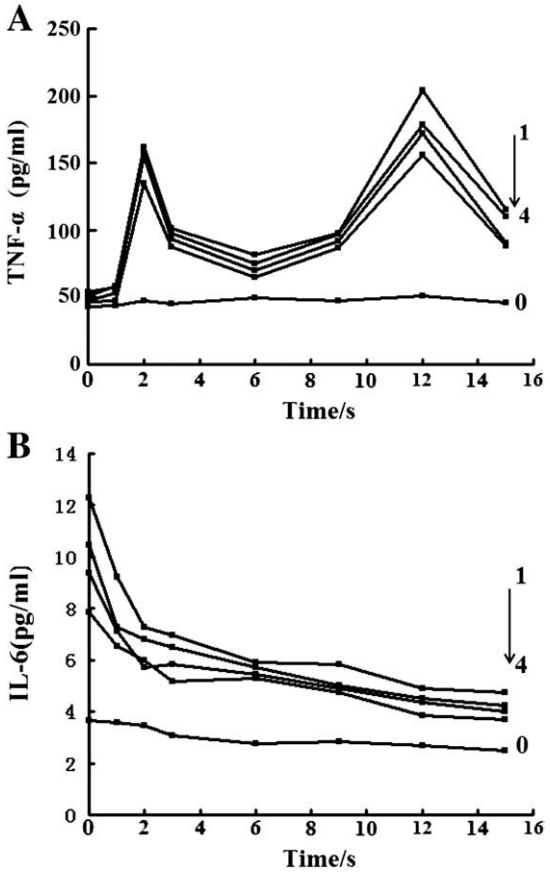

Fig. 5. Time series test of TNF-α, IL-6 level in supernatant of RAW264.7. The concentrations of TNF-α (A) and IL-6 (B) were measured at different time points (0, 1, 2, 3, 6, 9, 12 and 15 h) in RAW264.7 which were stimulated with HMGB1 (0.1 μg/mL) and different concentrations of heparin (0, 0.1, 1, and 10 U/L from 1 to 4). The cells which were not stimulated with HMGB1 were used as control group (0).

4. Discussion

HMGB1 has been identified as a late-acting mediator of endotoxin lethality [11]. Serum HMGB1 levels are high in patients with endotoxemia, hemorrhagic shock, acute lung injury, rheumatoid arthritis, and disseminated intravascular coagulation [24–26].

The cytokine activity of HMGB1 in many cell types has been well-documented. In cultured human primary macrophages/monocytes, HMGB1 stimulates the release of various proinflammatory cytokines, including TNF-α, IL-1α, IL-1β, IL-1RA, IL-6, IL-8, macrophage inflammatory protein (MIP)-1α, and MIP-1β, but not IL-10 and IL-12 [27]. In cultured human microvascular endothelial cells, the addition of HMGB1 induces the expression of adhesion molecules such as intercellular adhesion molecule (ICAM)-1, vascular cell adhesion molecule-1 (VCAM-1), and RAGE, as well as the release of TNF-α and IL-8, macrophage chemoattractant protein (MCP)-1, plasminogen activator inhibitor (PAI)-1, and tissue plasminogen activator (tPA). HMGB1 can also activate human neutrophils to produce proinflammatory mediators such as TNF-α, IL-1β, and IL-8, and it can also increase the permeability in cultured enterocytes via a nitric oxide (NO)-dependent pathway [27,28]. Hence, HMGB1 is a potent molecule that augments inflammatory response. Administration of anti-HMGB1 antibodies to endotoxemic animals can afford protection to the animals against endotoxin lethality. The blockade of HMGB1 activity attenuates the development and related organ dysfunctions in experimental severe acute pancreatitis (SAP).

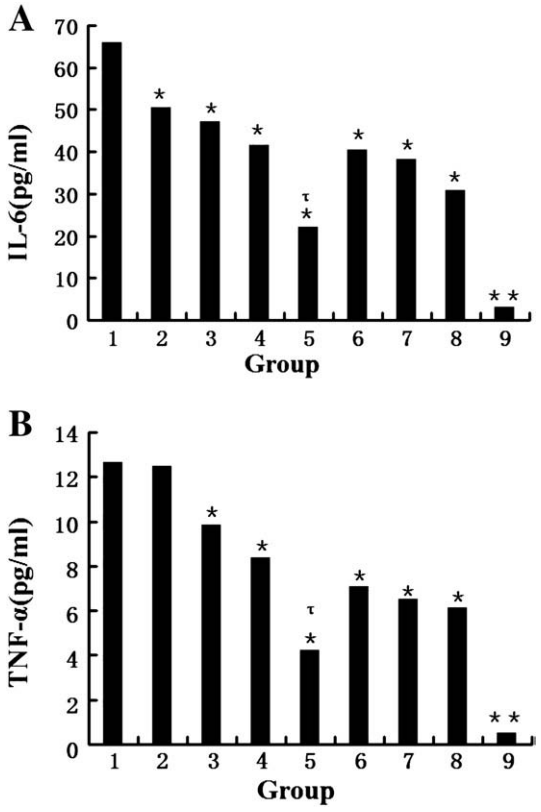

Fig. 6. Concentration of IL-6 and TNF-α in HUVEC supernatant. The levels of IL-6 (A) and TNF-α (B) were measured in HUVEC supernatants which were stimulated with HMGB1 (0.1 μg/mL) and different concentrations of heparin (0, 0.1, 1, 10, 50, 100, 1000 and 10,000 U/L from 1 to 8) for 24 h. Control group was not stimulated with HMGB1 as 9. *P<0.05 compared with group 1. τP<0.05 compared with the values in other groups (2–8). **P<0.01 compared with control group 9.

In addition to acting as a receptor of multiple ligands, RAGE also mediates the cytokine activity of HMGB1 in vascular endothelial cells, macrophages, and tumor cells [29,30]. The main consequences of the interaction of HMGB1 with RAGE are as follows: activation of the CDC42 and Rac guanosine triphosphatases that regulate cell motility and neurite outgrowth and activation of several mitogen-activated protein kinases (MAPKs); these events subsequently lead to activation of nuclear factor (NF)-κB [31]. The HMGB1/RAGE interaction leads to the phosphorylation of MAPKs (e.g., p38 and p42/44 kinases, stress-activated protein kinase/c-Jun N-terminal kinase, and ERK1/2) and the activation of NF-κB signaling pathway in cultured macrophages, neutrophils, and Caco-2 epithelial cells [32,33].

Heparin, a highly sulfated glycosaminoglycan, is widely used as an injectable anticoagulant and has the highest negative charge density among all biological molecules. Although used principally as an anticoagulant, heparin can also be used for anti-inflammatory, antitumor, and antianaphylactic purposes. However, the true physiological role of heparin in vivo remains unclear.

The comparison of fluorescence peaks of tryptophan and tyrosine between HMGB1 and free status revealed that the emission wavelength of tyrosine had a blue shift of about 12 nm while the emission wavelength of tryptophan had a blue shift of 21 nm. According to Chuang VT [34], the residues corresponding to these peaks could be assumed to be buried in the hydrophobic microenvironment of the peptide chain of HMGB1 (Fig. 1B, C). Heparin was mixed with HMGB1 in different concentrations, but these components had complicated interactions. For example, in the sample containing 50 U/L heparin, the α-helix content increased and β-pleated sheet content of HMGB1 reduced and the synchronous fluorescence spectrum showed a red shift. Therefore, tryptophan and tyrosine amino acid residues in the hydrophobic site were first exposed to the heteropolar environment, and consequently the fluorescence intensity was elevated. All these data indicated that heparin had changed the conformation of HMGB1, thereby causing a change in the fluorescence characteristics of HMGB1.

In this study, the amine-coupling method did not destroy the binding site of heparin and HMGB1. Further, it was confirmed that HMGB1 is a heparin-binding protein with high affinity; the affinity constant was $K_A = 2.22 \times 10^8\ L \cdot mol^{-1}$ and the equilibrium dissociation constant was $K_D = 4.5 \times 10^{-9}\ mol \cdot L^{-1}$. Interestingly, when the concentration of HMGB1 was 50 mg/L, even the highest concentration of heparin (10,000 U/L) did not reach saturation.

Since the changes in protein conformation can affect protein functions, we also elucidated the effect of changes in HMGB1 conformation on its affinity and its interaction with RAGE.

HMGB1 was considered as the ligand with one of the highest affinities for RAGE. In our experiment, the kinetic constants of HMGB1 and RAGE were determined to be $K_A = 1.02 \times 10^7\ L \cdot mol^{-1}$ and $K_D = 9.77 \times 10^{-8}\ mol \cdot L^{-1}$, which showed that HMGB1 and RAGE did bind with a very high affinity (Fig. 3A, B).

We used binding analysis to investigate the effect of different concentrations of heparin on the affinity of HMGB1/RAGE. The results showed that the RUs for HMGB1 and RAGE binding reduced from about 100 RU to about 50 RU after mixing with heparin. Hence, heparin could remarkably decrease the affinity of HMGB1/RAGE.

Furthermore, we obtained similar results in experiments on RAW264.7 cells. TNF-α and IL-6 levels declined after the addition of different concentrations of heparin. Further, 10 U/L of heparin had the most marked effect on the inhibition of TNF-α and IL-6 release.

To investigate the ability of heparin neutralizing HMGB1, we estimated both the levels of IL-6 and TNF-α in the supernatants of HUVEC. The levels of IL-6 and TNF-α were significantly decreased after treatment with heparin in different concentrations compared to control group ($P<0.05$). And reach the minimum at the level of 50 U/L ($P<0.05$). But the use of heparin was restricted for its side-effect such as bleeding, so the safe dose should not exceed 5000 U/L. In our test, different concentrations of heparin from 0 U/L to 10,000 U/L which already include the proper dosage in clinic were tested, then we found that, 50 U/L had the best effect of neutralization. so we proposed that heparin of 50 U/L could not only best inhibit the inflammation effect induced by HMGB1/RAGE combination, but also reduces the adverse reactions in the clinical application of heparin, such as bleeding, thrombocytopenia, osteoporosis and drug resistance and other side-effects.

Since heparin did not combine with RAGE, as observed in our study, it can be presumed that heparin had no effect on RAGE. Hence, the changes in RU values could be attributed to the heparin-induced conformation changes in HMGB1. It may be assumed that the conformation changes of HMGB1 occurred in the RAGE-binding site, which contains 2 tyrosines and is located between the amino acids 150 and 183.

In this study, the effect of heparin on the affinity of HMGB1 (50 mg/L) for RAGE did not show positive correlation with its concentration. Since heparin did not reach saturation even at a concentration of 10,000 U/L, its effect on HMGB1 might not be dose dependent. This result indicates that a low dose of heparin is probably sufficient to achieve the best anti-inflammatory effect. But whether heparin interacts with other receptors of HMGB1 still need a further investigation.

Acknowledgements

We gratefully acknowledge Huazhong University of Science and Technology Analysis and Testing Center (FP-6500 and J-810) and Life Sciences College of Hubei University (BIAcore 3000) for supporting the equipments. We thank Xiao-Man Gu, Hong Cheng (Huazhong University of Science and Technology Analysis and Testing Center)

and Si-Jing Jiang (Life Sciences College of Hubei University) for their technical assistance.

This work was supported by the National Natural Science Foundation of China (No. 30600593).

References

[1] Yamada S, Maruyama I. HMGB1, a novel inflammatory cytokine. Clin Chim Acta 2007;375(1–2):36–42.
[2] Read CM, Cary PD, Crane-Robinson C, Driscoll PC, Norman DG. Solution structure of a DNA-binding domain from HMG1. Nucleic Acids Res 1993;21:3427–36.
[3] Weir HM, Kraulis PJ, Hill CS, Raine AR, Laue ED, Thomas JO. Structure of the HMG box motif in the B-domain of HMG1. EMBO J 1993;12:1311–9.
[4] Cardin AD, Weintraub HJ. Molecular modeling of protein–glycosaminoglycan interactions. Arteriosclerosis 1989;9:21–32.
[5] Huttunen HJ, Fages C, Kuja-Panula J, Ridley AJ, Rauvala H. Receptor for advanced glycation end products-binding COOH-terminal motif of amphoterin inhibits invasive migration and metastasis. Cancer Res 2002;62:4805–11.
[6] Aizawa S, Nishino H, Saito K, Kimura K, Shirakawa H, Yoshida M. Stimulation of transcription in cultured cells by high mobility group protein 1: essential role of the acidic carboxyl-terminal region. Biochemistry 1994;33:14690–5.
[7] Banerjee S, Kundu TK. The acidic C-terminal domain and A-box of HMGB-1 regulates p53-mediated transcription. Nucleic Acids Res 2003;31:3236–47.
[8] Li J, Kokkola R, Tabibzadeh S, Yang R, Ochani M, Qiang X, et al. Structural basis for the proinflammatory cytokine activity of high mobility group box 1. Mol Med 2003;9:37–45.
[9] Johns EW. Studies on histones, 7: preparative methods for histone fractions from calf thymus. Biochem J 1964;92:55–9.
[10] Bustin M. Regulation of DNA-dependent activities by the functional motifs of the high-mobility-group chromosomal proteins. Mol Cell Biol 1999;19:5237–46.
[11] Wang H, Yang H, Czura CJ, Sama AE, Tracey KJ. HMGB1 as a late mediator of lethal systemic inflammation. Am J Respir Crit Care Med 2001;164:1768–73.
[12] Park JS, Svetkauskaite D, He Q, Kim JY, Strassheim D, Ishizaka A, et al. Involvement of toll-like receptors 2 and 4 in cellular activation by high mobility group box 1 protein. J Biol Chem 2004;279:7370–7.
[13] Yang H, Ochani M, Li J, Qiang X, Tanovic M, Harris HE, et al. Reversing established sepsis with antagonists of endogenous high-mobility group box 1. Proc Natl Acad Sci USA 2004;101:296–301.
[14] Brett J, Schmidt AM, Yan SD, Zou YS, Weidman E, Pinsky D, et al. Survey of the distribution of a newly characterized receptor for advanced glycation end products in tissues. Am J Pathol 1993;143:1699–712.
[15] Neeper M, Schmidt AM, Brett J, Yan SD, Wang F, Pan YC, et al. Cloning and expression of a cell surface receptor for advanced glycosylation end products of proteins. J Biol Chem 1992;267:14998–5004.
[16] Kislinger T, Fu C, Huber B, Qu W, Taguchi A, Du Yan S, et al. N(epsilon)-(carboxymethyl) lysine adducts of proteins are ligands for receptor for advanced glycation end products that activate cell signaling pathways and modulate gene expression. J Biol Chem 1999;274:31740–9.
[17] Rao CM. Synchronous scan fluorescence spectroscopy of proteins and human eye lenses. Biochem Biophys Res Commun 1991;176:1351–7.
[18] Chen YH, Yang JT, Chau KH. Determination of the helix and beta form of proteins in aqueous solution by circular dichroism. Biochemistry 1974;13(16):3350–9.
[19] Karlsson R, Michaelsson A, Mattsson L. Kinetic analysis of monoclonal antibody–antigen interactions with a new biosensor based analytical system. J Immunol Meth 15 Dec 1991;145(1–2):229–40.
[20] Lakowicz JR. Principles of fluorescence spectroscopy [M]. New York: Plenum Press; 1983. p. 342.
[21] Shutova T, Deikus G, Irrgang KD, Klimov VV, Renger G. Origin and properties of fluorescence emission from the extrinsic 33 kDa manganese stabilizing protein of higher plant water oxidizing complex. Biochim Biophys Acta 2001;1504(2–3):371–8.
[22] Muephy P, Nowak T, Lemon SM, Hilfenhaus J. Inactivation of hepatitis A virus by heat treatment in aqueous solution. J Med Virol 1993;41(1):61–4.
[23] Stenberg E, Persson B, Roos H. Quantitative determination of surface concentration of protein withsurface plasmon resonance by using radiolabeled proteins. J Colloid Interface Sci 1991;143:513–26.
[24] Ombrellino M, Wang H, Ajemian MS, Talhouk A, Scher LA, Friedman SG, et al. Increased serum concentrations of high-mobility-group protein 1 in haemorrhagic shock. Lancet 1999;354:1446–7.
[25] Abraham E, Arcaroli J, Carmody A, Wang H, Tracey KJ, et al. HMG-1 as a mediator of acute lung inflammation. J Immunol 2000;165:2950–4.
[26] Kokkola R, Sundberg E, Ulfgren AK, Palmblad K, Li J, Wang H, et al. High mobility group box chromosomal protein 1: a novel proinflammatory mediator in synovitis. Arthritis Rheum 2002;46:2598–603.
[27] Fiuza C, Bustin M, Talwar S, Tropea M, Gerstenberger E, Shelhamer JH, et al. Inflammation-promoting activity of HMGB1 on human microvascular endothelial cells. Blood 2003;101:2652–60.
[28] Treutiger CJ, Mullins GE, Johansson AS, Rouhiainen A, Rauvala HM, Erlandsson-Harris H, et al. High mobility group 1 B-box mediates activation of human endothelium. J Intern Med 2003;254:375–85.
[29] Taguchi A, Blood DC, del Toro G, Canet A, Lee DC, Qu W, et al. Blockade of RAGE-amphoterin signalling suppresses tumour growth and metastases. Nature 2000;405:354–60.
[30] Yang H, Wang H, Czura CJ, Tracey KJ. The cytokine activity of HMGB1. J Leukoc Biol 2005;78:1–8.
[31] Yan SD, Schmidt AM, Anderson GM, Zhang J, Brett J, Zou YS, et al. Enhanced cellular oxidant stress by the interaction of advanced glycation end products with their receptors/binding proteins. J Biol Chem 1994;269:9889–97.
[32] Lander HM, Tauras JM, Ogiste JS, Hori O, Moss RA, Schmidt AM. Activation of the receptor for advanced glycation end products triggers a p21(ras)-dependent mitogen-activated protein kinase pathway regulated by oxidant stress. J Biol Chem 1997;272:17810–4.
[33] Hazzalin CA, Mahadevan LC. MAPK-regulated transcription: a continuously variable gene switch? Nat Rev Mol Cell Biol 2002;3:30–40.
[34] Chuang VT, Otagiri M. Flunitrazepam, a 7-nitro-1, 4-benzodiazepine that is unable to bind to the indole-benzodiazepine site of human serum albumin. J Biochim Biophys Acta 2001;1546(2):337–45.